Microtubule Treadmilling in Vitro Investigated by Fluorescence Speckle and Confocal Microscopy

Sonia Grego, Viviana Cantillana, and E. D. Salmon
Department of Biology, University of North Carolina–Chapel Hill, Chapel Hill, North Carolina 27599-3280 USA

ABSTRACT Whether polarized treadmilling is an intrinsic property of microtubules assembled from pure tubulin has been controversial. We have tested this possibility by imaging the polymerization dynamics of individual microtubules in samples assembled to steady-state in vitro from porcine brain tubulin, using a 2% glycerol buffer to reduce dynamic instability. Fluorescence speckled microtubules were bound to the cover-glass surface by kinesin motors, and the assembly dynamics of plus and minus ends were recorded with a spinning-disk confocal fluorescence microscopy system. At steady-state assembly, 19% of the observed microtubules (n = 89) achieved treadmilling in a plus-to-minus direction, 34% in a minus-to-plus direction, 37% grew at both ends, and 10% just shortened. For the population of measured microtubules, the distribution of lengths remained unchanged while a 20% loss of original and 27% gain of new polymer occurred over the 20-min period of observation. The lack of polarity in the observed treadmilling indicates that stochastic differences in dynamic instability between plus and minus ends are responsible for polymer turnover at steady-state assembly, not unidirectional treadmilling. A Monte Carlo simulation of plus and minus end dynamics using measured dynamic instability parameters reproduces our experimental results and the amount of steady-state polymer turnover reported by previous biochemical assays.

INTRODUCTION

For microtubules assembled in vitro from pure tubulin, a dominant aspect of assembly and disassembly is dynamic instability at microtubule plus and minus ends consisting mainly of stochastic and abrupt switches between persistent growing and persistent shortening phases (Fig. 1 *A*) (Mitchison and Kirschner, 1984; Walker et al., 1988; Inoué and Salmon, 1995; Desai and Mitchison, 1997). Dynamic instability is produced by the hydrolysis of GTP bound to tubulin after association into a microtubule end. This hydrolysis produces a core of GDP–tubulin within the microtubule lattice. A growing end is proposed to be stabilized mainly by a tubulin–GTP cap (Desai and Mitchison, 1997). When this cap is lost, an end has a high probability of switching (catastrophe) to the shortening state where tubulin–GDP dimers at the tip are able to peel outward away from the lattice and rapidly dissociate (Tran et al., 1997). Tubulin–GDP dissociation persists until the end either regains a stabilizing tubulin–GTP cap and switches back (rescue) to growth or shortens completely, causing the microtubule to disappear. In animal cells during mitosis and interphase, microtubule growth occurs at plus ends, and microtubule assembly is dominated by plus-end dynamic instability. Minus ends do not exhibit growth and are often stabilized by complexes such as the nucleation sites at centrosomes and spindle poles (Inoué and Salmon, 1995; Desai and Mitchison, 1997).

Another way the energetics of GTP hydrolysis can influence microtubule assembly is by producing treadmilling. Treadmilling is polarized head-to-tail polymerization, with persistent growth from one end and shrinking from the other (Fig. 1 *B*). There have been two proposals for the mechanism of treadmilling: the Wegner model and differential dynamic instability between the two ends. The Wegner model for treadmilling was initially proposed for actin filament assembly (Wegner, 1976) and applied to microtubule assembly (Margolis and Wilson 1978, 1998; Bergen and Borisy, 1980; Margolis, 1981) before the discovery of dynamic instability (Mitchison and Kirschner, 1984). It assumes that there is only one single continuous phase of association of tubulin–GTP and dissociation of tubulin–GDP taking place at an end (no shortening phase). GTP hydrolysis upon subunit binding to an end allows the critical tubulin concentrations for growth at opposite ends to be different. If the dimer pool concentration is at an intermediate value between the critical concentrations of the two ends, the end with the lower critical concentration will persistently grow while the end with the higher critical concentration will persistently shorten (Margolis and Wilson, 1998). For microtubule ends capable of dynamic instability (i.e., exhibiting shortening phases), differences in the contributions of the growth and shortening phases between the two ends provide another way to bias one end into net growth while the other end is biased into net shorten at steady-state assembly (Walker et al., 1988; Waterman-Storer and Salmon, 1997a). Treadmilling will occur if the growth phase is dominant at one end while the shortening phase is dominant at the other end. It should be noted that there has been a semantic problem with the definition of treadmilling in this field. When some people say "treadmilling" they mean the Wegner model (Margolis and Wilson,

Received for publication 20 February 2001 and in final form 4 April 2001.
Address reprint requests to Address correspondence to E. D. Salmon, Dept. of Biology CB# 3280, University of North Carolina–Chapel Hill, Chapel Hill, NC 27599-3280. Tel.: 919-962-2265; Fax: 919-962-1625; E-mail: tsalmon@email.unc.edu.

0006-3495/01/07/66/13 $2.00

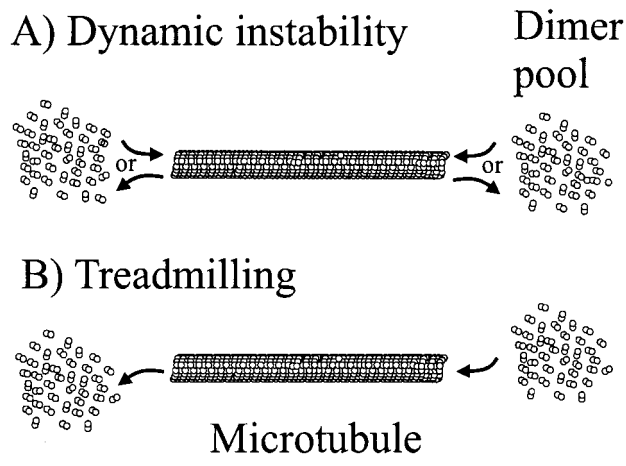

FIGURE 1 Comparison of two views of microtubules assembly. (*A*) Microtubule dynamic instability where assembly at each end is dominated by abrupt changes between persistent states of growth and shortening. (*B*) Polarized treadmilling produced by head-to-tail polymerization with persistent growth at one end and shortening at the other.

1998). Others mean any kind of assembly behavior with net assembly at one end and net disassembly at the other no matter what other protein factor may be involved (Waterman-Storer and Salmon, 1997a; Rodionov and Borisy, 1997; Rodionov et al., 1999)

There is evidence that treadmilling with net plus-end growth and minus-end shortening can occur at significant rates in living cells when microtubule minus ends are free of nucleation centers like centrosomes (reviewed in Waterman-Storer and Salmon, 1997a; Rodionov et al., 1999). Mitotic microtubules have been shown to have a poleward rate of lattice movement between 0.3 and 2 μm/min, depending on the species, with a net addition of subunits at their plus ends near the middle of the spindle and loss of subunits at their minus ends at the spindle poles (Mitchison, 1989; Mitchison and Salmon, 1992; Zhai et al., 1995; Desai et al., 1998). The steady poleward movement of mitotic microtubules has been called "flux" to differentiate it from treadmilling because it may involve other sources of energy input, such as microtubule motors, beyond the energetics of hydrolysis of GTP bound to tubulin (Mitchison, 1989; Desai et al., 1998). Treadmilling has also been observed during interphase for microtubules with minus ends released from the centrosome in melanophores and fibroblast cells with net growth at the plus end at the very high velocity of 12 μm/min and shortening at the minus ends at similar velocities (Rodionov and Borisy, 1997; Rodionov et al., 1999). Waterman-Storer and Salmon (1997b) observed treadmilling of microtubules in epithelial cells where the plus ends exhibited dynamic instability with net growth but the minus ends exhibited either shortening or pauses. Because fast growth and shortening rates are typical of the dynamic instability of microtubules in living cells, these studies suggested that treadmilling is facilitated by nontubulin factors that selectively promote growth at plus ends and block growth and promote shortening at the minus end (Waterman-Storer and Salmon, 1997a,b; Rodionov et al., 1999)

A controversial issue is whether microtubules assembled from pure tubulin exhibit intrinsic polarized treadmilling. Margolis and Wilson (1978) initially reported evidence for microtubule treadmilling based on biochemical assays for the gain and loss of tubulin subunits in microtubules at steady-state assembly in vitro. Bergen and Borisy (1980) measured nucleated microtubule growth for plus and minus ends and predicted polarized treadmilling in a plus direction at slow velocities, 0.05 μm/min, for microtubules assembled with a mixture of brain microtubule-associated proteins (MAPs). In a subsequent study, Hotani and Horio (1988) used dark field microscopy to observe individual microtubules and analyze the relationship between treadmilling and dynamic instability. They concluded that microtubules assembled from pure mammalian brain tubulin exhibit dynamic instability. Microtubules assembled with brain MAPs were shown to exhibit no shortening phases and a slight treadmilling at 0.015 μm/min with continuous growth at the plus end and shortening at the minus end near steady-state assembly. Kristofferson et al. (1986) visualized many individual microtubules after they were assembled to steady-state using fixed-time point immunofluorescence assays and biotinylated tubulin as a lattice marker. On the basis of classification of labeling patterns, they found no evidence for treadmilling for pure tubulin microtubules whose assembly was dominated by dynamic instability in standard Pipes assembly buffer. Addition of 30% glycerol to the buffer made microtubules much less dynamic (when viewed over 200 min) and 30% of the microtubules could have been in a treadmilling state of unknown polarity because marker incorporation occurred only at one end. However, the main point of their measurements was that the majority of the microtubules grew at both ends, thereby excluding treadmilling as a major mechanism of microtubule dynamics for microtubules assembled from pure tubulin. Fygenson et al. (1994) also concluded that treadmilling is not a significant property of pure tubulin microtubules. Their conclusion was based on an analysis of the occupancy of nucleation sites for plus and minus ends over a range of tubulin concentration and temperature that indicated that both plus and minus ends have very similar critical concentrations.

More recently, Panda et al. (1999) have re-addressed the issue of intrinsic treadmilling for pure-tubulin microtubules. They suppressed the shortening phases of dynamic instability by adding 2% glycerol to the microtubule assembly buffer. Subunit incorporation and loss per microtubule were estimated by biochemical assays of the rate of radiolabeled GTP-tubulin incorporation and loss from microtubules at steady-state assembly in combination with length histograms. They reported rates of 0.32 μm/min for gain and 0.26 μm/min for loss of tubulin per microtubule. After corrections for potential contributions from the suppressed

dynamic instability, a treadmilling rate of 0.2 μm/min was calculated. This rate was proposed to reflect polarized Wegner head-to-tail treadmilling (Fig. 1 *B*) and not the results of differences in dynamic instability between plus and minus ends (Fig. 1 *A*). A treadmilling rate of 0.2 μm/min is significant because it is much higher than predicted from the previous in vitro studies with pure tubulin (Kristofferson et al., 1986; Hotani and Horio, 1988; Fygenson et al., 1994) and because it could make significant contributions to the 0.3 to 0.5 μm/min velocity of kinetochore microtubule poleward flux in mammalian tissue cells (Mitchison, 1989; Mitchison and Salmon, 1992; Zhai and Borisy, 1995; Waters et al., 1996).

In this paper, we investigate whether pure tubulin microtubules exhibit polarized treadmilling by using new methods for imaging the assembly dynamics of the plus and minus ends of individual microtubules. Microtubules were assembled to near steady-state using the same glycerol stabilization buffer described by Panda et al. (1999) and a tubulin dimer pool containing a small (2%) fraction of X-rhodamine-labeled tubulin to produce fluorescent speckles along the microtubules (Waterman-Storer and Salmon, 1997b, 1998). Low concentrations of kinesin motors were used to bind microtubules to the inner surface of a slide–coverslip assembly chamber. Slow plus-end-directed translocation of the microtubules by the kinesin motors identified the polarity of microtubule ends in time-lapse records obtained with a spinning-disk confocal fluorescence microscopy system that rejected the out-of-focus fluorescence from tubulin and microtubules in the 70-μm-deep chamber. Growth and shortening at microtubule ends were measured relative to fluorescent speckles in the microtubule lattice. We found that, at steady-state assembly, both plus and minus ends exhibited the growth and shortening phases of dynamic instability, although periods of pause with no net growth or shortening also occurred. Over an average observation time of 17 min, some microtubules achieved treadmilling in a plus-to-minus direction, others in a minus-to-plus direction, and other microtubules either grew or shortened at both ends. We attributed this behavior to the stochastic aspects of dynamic instability and modeled it with a Monte Carlo simulation using the experimental parameters measured for the dynamic instability at plus and minus ends. The simulation results showed a population near steady-state assembly whose dynamics reproduced the experimental data. This imaging assay is a powerful tool to judge unambiguously treadmilling and is susceptible to introduction of factors such as MAPs, motors, or other factors that could polarize microtubule assembly dynamics.

MATERIALS AND METHODS

Microtubule assembly

Tubulin was purified from porcine brain by cycles of polymerization, depolymerization, and differential centrifugation, followed by phosphocellulose chromatography as described in Walker et al. (1988). Tubulin (stock concentration of 109 μM) was stored at −80°C until use. Tubulin was labeled with X-rhodamine succinimidyl ester at a molar dye:protein ratio of 2.5:1 using the methods of Waterman-Storer and Salmon (1997) and stored at a concentration 170 μM at −80°C until use.

Microtubules were assembled to near steady state according to a procedure similar to that described in Panda et al. (1999) except that we added fluorescent tubulin to provide lattice marks. To prepare microtubule seeds for nucleation, 30 μM tubulin (10% X-rhodamine labeled) was polymerized in PME buffer (100 mM Pipes/1 mM Mg^{2+}/1 mM EGTA with 1 mM GTP) containing 10% glycerol (vol/vol), 5 mM NaCl, and 1 mM GTP for 30 min at 30°C. After 30 min of polymerization, seeds were sheared by passage (up to 10 times) through the needle of a 50-μl Hamilton syringe. Tubulin mixtures containing a 2% fraction of X-rhodamine-labeled tubulin were diluted in PME containing 1 mM GTP, 5 mM NaCl, 10 μM ATP and an antifade mixture (10 μg/ml catalase, 5 μg/ml glucose oxidase, 10 mM D-glucose, and 1 mM DTT). Seeds were then added in ratio 1:5 vol/vol to the mixture warmed to room temperature. The final concentration of tubulin was 15 μM and the final glycerol concentration was 2%. Note that NaCl and ATP were present in the sample buffer at low concentrations to support slow kinesin motility in the microscope polarity assay. Microtubules were polymerized for 30 min at 30°C to achieve near steady-state assembly (Panda et al., 1999).

Slide–coverslip chamber preparation

Slide–coverslip chambers were made by placing a #1.5 coverslip on two strips of double stick tape set about 3 mm apart on a slide to make a perfusion chamber with a 70-μm-thick channel. Kinesin protein (KR01, Cytoskeleton, Denver, CO) at concentration of 200 μg/ml was perfused into the chamber and incubated for 10 min in a humidified dish. This protein construct consists of the first 685 amino acids of *Drosophila* kinesin including the motor head and stalk, making the protein competent for binding microtubules to the coverslip inner surface and producing ATP-driven motor activity. Next, α-casein (10 mg/ml) was perfused in the chamber to prevent unspecific binding of tubulin to glass. After 5 min, the chamber was rinsed with warm PME and microtubules, after assembly at 30°C for 30 min, were perfused into the chamber. The sample was sealed with VALAP (1:1:1 vasoline:lanolin:paraffin) and quickly put on the microscope stage heated at 30°C.

Image acquisition

Time-lapse images were acquired by a Yokogawa spinning-disk confocal system. The spinning-disk system Yokogawa CS10 (Perkin-Elmer Life Sciences Wallac, Gaithersburg, MD) was mounted to the camera port of Nikon TE300 inverted scope. An air-cooled Ar/Kr laser (60 mW, Melles Griot, Carlsbad, CA) was fiber-optically coupled to the spinning head, and filter wheels selected illumination at 568 nm. Digital images were acquired by a 16-bit cooled CCD camera with extended sensitivity in the red (Orca ER, Hamamatsu Photonics, Bridgewater, NJ). Focus was controlled by a remote focusing accessory (Nikon) and was manually corrected for stage drift, a crucial need for the visualization of microtubules, which are only 25 nm in diameter. The acquisition system was controlled by MetaMorph software (Universal Imaging Corp., West Chester, PA) in a PC computer. Fluorescence images were acquired with 1-s exposure at 30-s intervals. The stage was maintained at 30°C by means of an air-stream incubator (Nevtek, Burnsville, VA). Images were stored on the hard disk and archived on CD-Rom for analysis.

Data analysis

In the acquired images, the presence of fluorescent speckles and strongly labeled seeds along the lattice allowed us to distinguish unambiguously

translation from growth and shortening. All the position measurements of the microtubule ends were made by using the motion analysis function of the MetaMorph software. A pixel-to-distance conversion factor was determined by means of 10-μm stage micrometer. The distance of the plus and minus ends from a fluorescent mark on the lattice was recorded for all the in-focus time-lapse images, transferred to a Microsoft Excel spreadsheet, and a time-series plotted for each end.

For the analysis of the assembly kinetics, we considered the microtubule in a growing state if it elongated more than 0.5 μm and shortening if it shrank by more than 0.5 μm. The periods during which length variation was smaller than 0.5 μm were considered as a third possible state of the microtubule end, the pause.

Estimation of the active kinesin motor surface concentration in the coverslip-slide chambers

We used 200 μg/ml of motor protein, equivalent to ~3000 molecules/μm^3. Considerations have been made (Howard et al., 1993) about diffusion of protein, incubation time, and limited binding capacity to the glass that yielded an estimate for the surface concentration of several thousands of motors/μm^2. However, only a small fraction of the adsorbed motor was expected to be active. Duke et al. (1995) estimated that, at a density of surface motor below 50 motors/μm^2, the leading edge of bound microtubules is subject to lateral fluctuations. Under our assembly conditions, we did not observe any lateral fluctuations of the leading edge of translocating microtubules, but we observed them when we reduced the motor concentration by a factor 10. We concluded from this assay that the concentration of active motors in our assembly assay was a value between 50 and 500 active motors/μm^2. This implied that the area covered by a 25-nm-diameter microtubule contained between 1.2 and 12 motors/μm. Because there are 1625 dimers/μm in a microtubule, only 1 dimer out of 1000 or 100 was interacting with a motor.

RESULTS

Imaging the assembly dynamics of plus and minus microtubule ends at steady-state assembly

Microtubules were assembled in vitro in a test tube at 30°C from pure porcine tubulin essentially as described by Panda et al. (1999) and transferred to a slide–coverslip chamber by perfusion. To put fluorescent marks within the microtubule lattice, the seeds used to nucleate microtubule assembly were made with a 10% fraction of X-rhodamine-labeled tubulin, whereas the assembly of microtubules nucleated from the fluorescent seeds was made with ~2% fraction of X-rhodamine-labeled tubulin. Some of the microtubules in the 70-μm-thick chamber were held to the coverslip surface by a low density of kinesin motors bound to the surface as diagrammed in Fig. 2 *A* and shown in Fig. 2, *C* and *D*. The 2% fraction of X-rhodamine-labeled tubulin produced a fluorescent speckle distribution all along the lengths of microtubules (Fig. 2 *C*), which we could use as position marks along the microtubule lattice as described by Waterman-Storer and Salmon (1998). These fluorescent speckle microtubules were invisible by standard wide-field epifluorescence microscopy because of the high level of out-of-focus fluorescence generated by the fluorescent tubulin and microtubules within the 70-μm-thick assembly chamber (Fig. 2 *D*). This out-of-focus fluorescence was removed by imaging the coverslip-bound microtubules with a Yokogawa CSU-10 spinning-disk confocal attachment between the side port of a Nikon inverted microscope and the Hamamatsu Orca ER cooled CCD camera (Figs. 2 *B* and 3). This imaging system produced 900 $\times$ 900 pixels images corresponding to a field of view of 96 $\times$ 96 μm^2 using a 63$\times$ objective. This gave sufficient resolution to detect the fluorescent speckles along the microtubule lattice (Waterman-Storer and Salmon, 1998) in the digital images.

Images of the same microtubules were acquired for a relatively long period of time, 15–20 min, to study the potential treadmilling of a microtubule at a rate of 0.2 μm/min as predicted by Panda et al. (1999). Because of photobleaching limitations, digital images were captured every 30 s, with the drawback that the dynamic behaviors of individual ends were sampled over a relatively long period compared with previous studies with shorter sampling times (Walker et al., 1988, 1991; Tran et al., 1997b). As a result, we expected to bias our determination of velocities of growth and shortening toward slower values. However, measurements of the rates of switching between dynamic instability states of growth, shortening, or pause (see below) were biased in the same way so that the overall description for $n = 89$ microtubules analyzed was consistent. For example, by sampling over a shorter period of time, 10 s, we occasionally observed (30% of the cases) that we underestimated the shortening velocity, but this was compensated by an overestimation of the period in shortening. We did not see any new growth and shortening phases not detected by the 30 s interval data.

To identify plus and minus ends accurately, we added 10 μM ATP and 5 mM NaCl to support slow kinesin motility in addition to the 1 mM GTP needed to support microtubule assembly. The fluorescent speckled microtubules moved across the coverslip surface in a minus-end direction as diagrammed in Fig. 2 *A* and shown in Fig. 3. In this way, the motor activity defined the polarity of the microtubules but the translation was slow enough to allow time-lapse imaging of both ends of a microtubule for typically 15–20 min before the microtubule left the field of view. In presence of 10 μM ATP in the assembly buffer, microtubule translocation occurred with average velocity 0.9 $\pm$ 0.4 μm/min.

Analysis of plus- and minus-end assembly dynamics for individual microtubules at steady-state assembly

The microtubule population analyzed was near steady-state assembly in the slide–coverslip chamber as shown by the similarity of the histograms (Fig. 4) of microtubule lengths measured at the beginning and the end of analysis (the average time interval was 17 min, the average length was 25 μm). The total length of the polymer measured increased during the acquisition period by only 5%. We were able to measure 89 microtubules from 9 chamber preparations

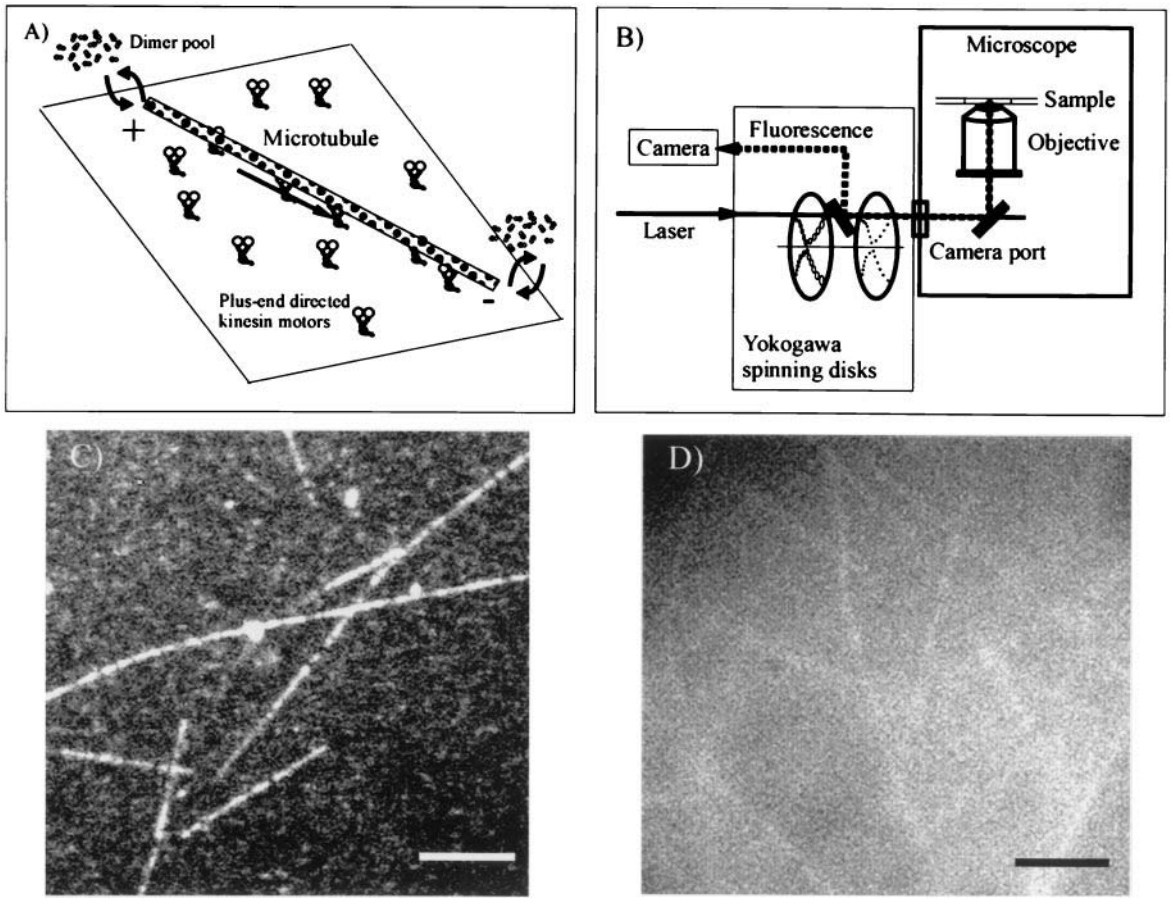

FIGURE 2 Slide–coverslip chamber assay for the assembly dynamics at plus and minus ends of individual microtubules using spinning-disk confocal and fluorescence speckle microscopy. (*A*) Microtubule polarity assay: the inner surface of the coverslip of the perfusion chamber is coated with kinesin motors to translocate bound microtubules toward their minus ends at slow velocities. (*B*) Experimental setup: images of fluorescent speckled microtubules are recorded using a 63X/1.4NA objective and a sensitive cooled CCD camera coupled to a Yokogawa spinning-disk confocal scanner (CSU10) mounted to the camera port of a Nikon TE300 inverted microscope (see text for details). (*C*) Typical confocal image of fluorescent speckled microtubules in the assay. Scale bar = 5 μm. (*D*) A wide-field fluorescence image of a similar microtubule preparation for comparison. Scale bar = 5 μm.

whose entire length remained in the 96 × 96 μm^2 field of view during the analysis period.

Measurements of the assembly at either plus or minus ends were made relative to fluorescent speckle marks on the microtubule lattice or one edge of the bright fluorescent nucleation seed in the middle of the microtubule (*arrows* in Fig. 3). Figure 5 shows representative plots of plus- and minus-end assembly behavior for individual microtubules. Our accuracy of repetitive measurements was ± 0.3 μm for each point in the graphs. Therefore, the switches between growth, shortening, or pause phases seen in the plots are mostly real and not an artifact of measurement inaccuracies. Positive and negative slopes represent growth and shortening phases in the graphs of Fig. 5, respectively. There were also periods where an end did not appear to be persisting in either growth or shortening for more than 0.5 μm. As defined by Walker et al., 1988, we term these periods pauses (see P region on lower right graph in Fig. 5).

As shown in Fig. 5, there was great variability in dynamic behavior for both plus or minus ends. The assembly dynamics at both ends was dominated by dynamic instability, though suppressed by the presence of the 2% glycerol because no microtubules shortened to complete disappearance. We never observed one microtubule end continuously growing while the other end was continuously shortening as predicted by the polarized head-to-tail treadmilling hypothesis (Fig. 1 *B*).

Another possibility was that treadmilling could be produced if the dynamic instability of one end was biased toward net growth while the other end was biased toward net shortening. We therefore classified microtubule end behavior according to the net growth or shortening that occurred between the beginning and the end of the time series, ignoring the intermediate position fluctuations. Individual examples are shown in Fig. 5, whereas Fig. 6 *A* summarizes the net changes in length at plus and minus ends for the 89 microtubules analyzed. We found that 53% of the population exhibited treadmilling within the observation period, but this treadmilling was not unidirectional: 19% of the microtubules showed net growth at the plus end

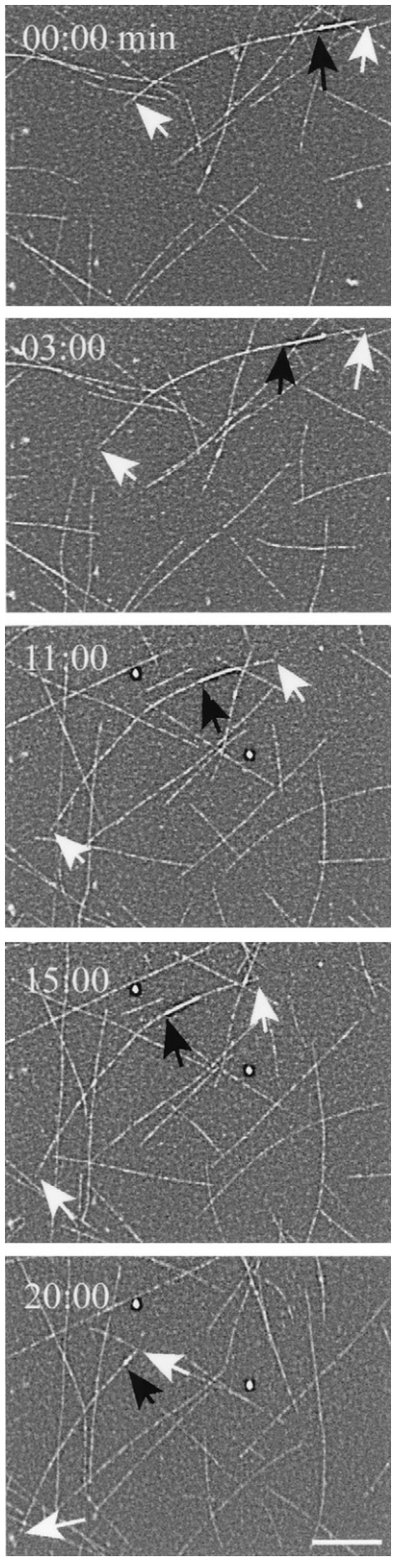

FIGURE 3 Time-lapse images of fluorescent speckled microtubules in the slide–coverslip assembly chamber near steady-state assembly. In each frame, the white arrows point to the dynamic ends of microtubule, and the black arrow points to the lattice mark (a 10% X-rhodamine-labeled seed in this case) used to distinguish translocation from end assembly dynamics. Scale bar = 10 μm.

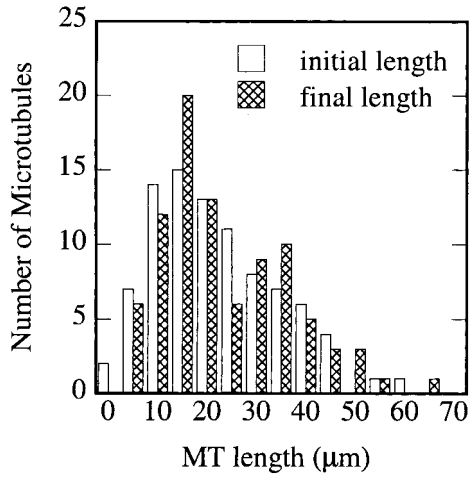

FIGURE 4 Histograms of the length distributions of analyzed microtubules (n = 89) at the beginning and at the end of their time series. The average time of observation was ~17 min. Microtubules that did not remain completely in the 96 × 96 μm^2 field of view during the observation period were not analyzed.

and shortening at the minus end and 34% of the them showed exactly the opposite. The other 47% of the population of microtubules analyzed exhibited either net growth (37%) or net shortening (10%) at both ends. The length variation averaged over all the microtubules was slightly positive at both microtubule ends, 0.08 ± 0.04 μm/min at the plus end and 0.034 ± 0.02 μm/min at the minus end. For the microtubules that exhibited net treadmilling in either direction, the average velocity of net growth at one end (the thin linear regression lines through the plots in Fig. 5) were rarely equal for plus and minus ends and varied from 0.1 to 0.5 μm/min. The heterogeneity in growth and shortening velocities seen in the plots in Fig. 5 is typical of microtubules assembled in vitro from pure brain tubulin, but the origins of this heterogeneity are poorly understood (Gildersleeve et al., 1992).

Estimation of gain of new polymer and loss of original polymer

Key data used by Panda et al. (1999) in support of microtubule treadmilling was the finding from biochemical assays that, near steady-state assembly, there was a linear loss of original polymer and a linear gain of new polymer at similar rates, a result expected from polarized head-to-tail treadmilling (Fig. 1 *B*). In our studies, we have information about plus and minus end-length changes for individual microtubules, which, when considered altogether, provide a reliable way to measure the rate of loss of original and gain of new polymer.

One approach to exploit the information contained in the individual microtubule time series consists of showing the entire loss of original and gain of new polymer that occurred

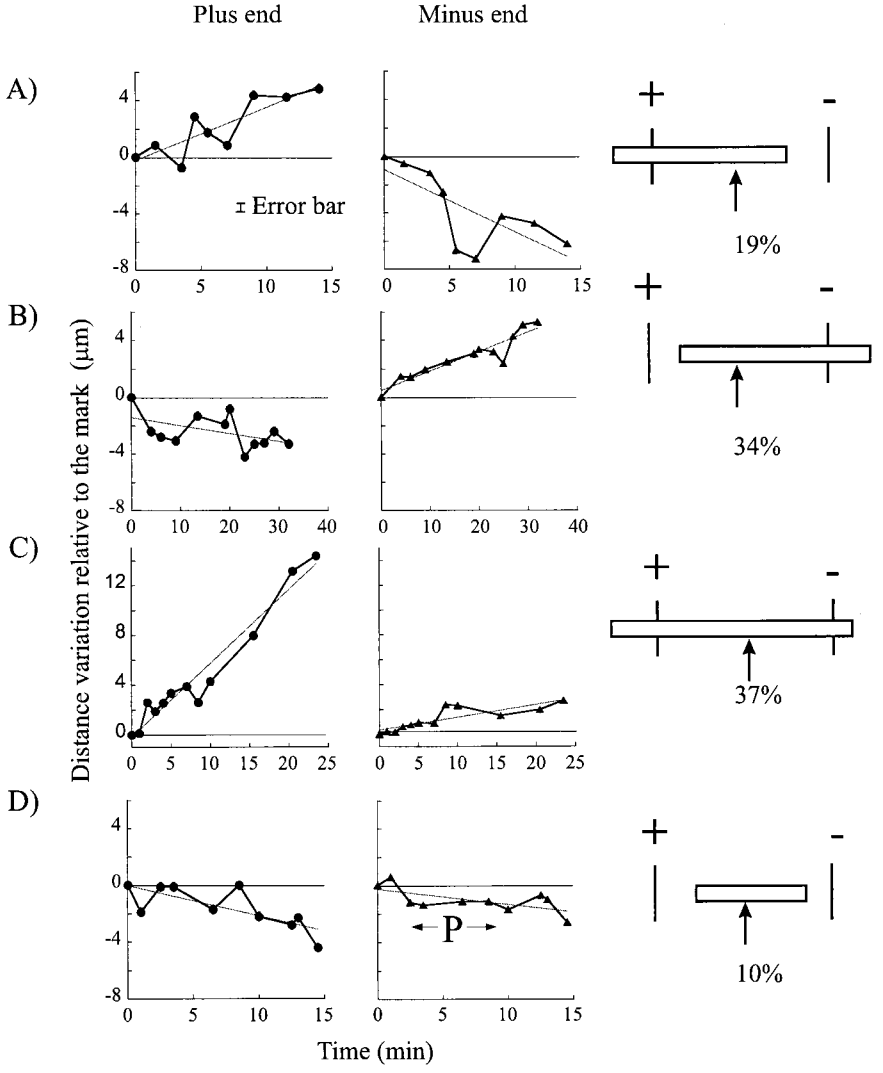

FIGURE 5 Examples of the dynamic assembly behavior at plus and minus ends of four different microtubules illustrating the four different behaviors observed in the microtubule population: (*A*) growth at the plus end and shortening at the minus end producing treadmilling toward the plus direction (19%); (*B*) growth at the minus end and shortening at the plus end producing treadmilling toward the minus end (34%); (*C*) growth at both ends (37%); and (*D*) shortening at both ends (10%). The thin lines are linear regression of the data.

for each microtubule analyzed in the population independent of the different durations analyzed for each microtubule (range 10–30 min). Original polymer is shown as *thin lines* whereas new polymer is shown as *thick lines* in Fig. 6 *A*. In this plot, the initial position of the plus ends is set at $+12.5$ μm, whereas the initial positions of the minus ends is set at -12.5 μm independent of the original lengths of the microtubules in the population. The total gain (summed over all the microtubules) in new polymer was 517 μm, which represented a gain of 23.6% when divided by the total initial length, 2187 μm, of the polymer population. In an analogous way, the total loss of original polymer was 388 μm, which represented a percentage loss of 18%. The average rates of gain of new and loss of old polymer were 0.37 ± 0.06 μm/min and 0.26 ± 0.04 (SEM) calculated as length/(number microtubules $\times$ average observation time).

In another approach, we calculated original polymer loss and new polymer gain at each end as a function of time. Original polymer loss was obtained by the difference between initial position and the position of maximal shortening that occurred from the beginning of the analysis. New polymer gain was measured by the difference between the current position of the end and the position of maximum polymer loss (not simply the initial position). The loss of original and gain of new polymer per microtubule was obtained by summing the measured values for both ends. Because of the random nature of the gain and loss events (Figs. 5 and 6 *A*), the total trend is meaningful only if the number of microtubules in the population analyzed is sufficiently high. Figure 7 *A* shows that, during the first 12 min of analysis, both loss of original and gain of new polymer followed linear kinetics at about 0.37 μm/min; beyond 12

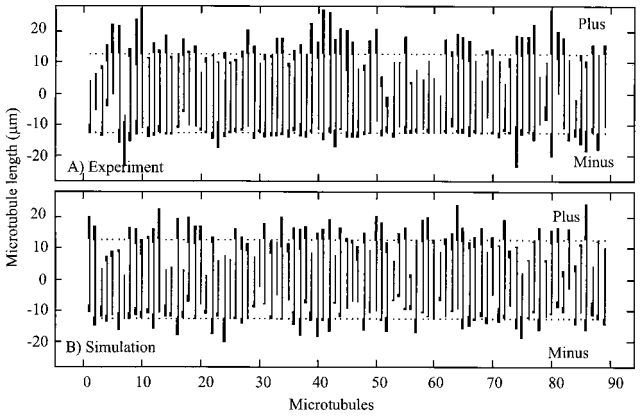

FIGURE 6 Comparisons of the net changes in length, net loss of original polymer, and net gain of new polymer, at plus and minus ends for the 89 microtubules analyzed (*A*) in our experiments and (*B*) by Monte Carlo computer simulation using the measured dynamic instability parameters (Table 1) for a 17-min period. In this analysis, the initial microtubule lengths are ignored, and, for each microtubule, the initial positions of the plus ends are set to $+12.5$ μm and the initial positions of the minus ends are set to -12.5 μm (*dotted horizontal lines*). The ends of the vertical lines represent the positions of the plus and minus ends at the end of (*A*) the analysis or (*B*) simulation. Plus ends grew in the plus direction and minus ends grew in a minus direction. The thick regions of the vertical lines correspond to gain of new polymer, and the distance between the bases of the thick regions and the initial end positions (*dotted horizontal lines*) show loss of original polymer.

min, the plots became irregular because of a decreasing number of microtubules in the population analyzed for longer durations. Nevertheless, note that linear kinetics for the loss of original and gain of new polymer is exhibited by the initial population of microtubules, although they did not exhibit polarized head-to-tail treadmilling, but either grew or shortened randomly among the plus and minus ends (Figs. 5 and 6 *A*).

Parameters of dynamic instability for plus and minus ends near steady-state assembly

The parameters of dynamic instability traditionally consist of the velocities of growth and shortening and frequencies of catastrophe (a switch from growth to shortening phase) and rescue (a switch from shortening to growth) (Inoué and Salmon 1995, Desai and Mitchison, 1997). In the 2% glycerol assembly buffer, the plus end was the faster growing end, which is typical of microtubule assembly in general (Inoué and Salmon, 1995; Desai and Mitchison, 1997). The average velocities for growth at the plus and minus ends were 0.7 ± 0.07 μm/min and 0.47 ± 0.08 μm/min, and the time spent in the growing phase was 53% and 45%, respectively (Table 1). The average shortening velocities at the plus and minus ends were 1.0 ± 0.2 and 0.6 ± 0.1 μm/min, and the time spent in shortening was 31% and 28%, respectively (Table 1). The 2% glycerol substantially decreased the rate of shortening at either end in comparison to the 20–30-μm/min shortening velocities typical of pure tubulin microtubules in assembly buffer without glycerol (Walker et al., 1988, 1989). None of the 89 microtubules analyzed were seen to shorten without rescue during our period of analysis. The growth and shortening velocities were measured as the average of the growth and shortening slopes, respectively, in the time series, weighted by the fraction of total time spent with each slope (Table 1). The uncertainty in velocity is the standard error mean.

At steady-state assembly, we also observed significant periods of pause where an end did not persist in either growth or shortening for more than 0.5 μm. With few exceptions (Toso et al., 1993), occasional periods of pause have been observed for pure tubulin microtubules when assembled in buffers without glycerol (Walker et al., 1988), or not observed at all (Fygenson et al., 1994; Gildersleeve et al., 1992; Vasquez et al., 1997). As a result, pauses have been previously neglected by modeling because of their infrequency. In the 2% glycerol assembly buffer used in our studies, pausing did occur for a significant fraction of the observed time: 16% for the plus end and 27% for the minus end.

Pauses represented a state of microtubule assembly too frequent to be neglected. Therefore, we have characterized microtubule dynamic instability by treating pause as a third state of the end. In our model, an end switches among three persistent states or phases: growth (G), shortening (S), and pause (P) (Fig. 8). Our measured transition frequencies among these three states are reported in Table 1 for plus and minus ends and defined as k_{i-j} equals the number of event switches from state i to state j divided by the total time spent in the i state. For example, k_{g-s} is the parameter traditionally called catastrophe frequency. Errors were calculated assuming a Poissonian distribution of the switching events. For the cases where data were available, we measured the transition rates k_{p-g} and k_{p-s} as functions of the state the microtubule end was exhibiting before entering the pause state. The statistic available was limited (an average of 10 events per situation) and showed values of k_{p-g} and k_{p-s} that were similar for ends that were growing or shortening before switching to pause. The contribution of all the observed pause states was summed to obtain the values k_{p-g} and k_{p-s} reported in Table 1.

Monte Carlo simulation of microtubule assembly at steady state from measured parameters of dynamic instability

Monte Carlo simulations were accomplished using MatLab software (version 6.0, MathWorks Inc., Natick, MA). Plus and minus ends were assumed to persist in one of the three dynamic instability states, growth (G), shortening (S), or pause (P), until abruptly switching to another state (Fig. 8), as described above for the experimental population of mi-

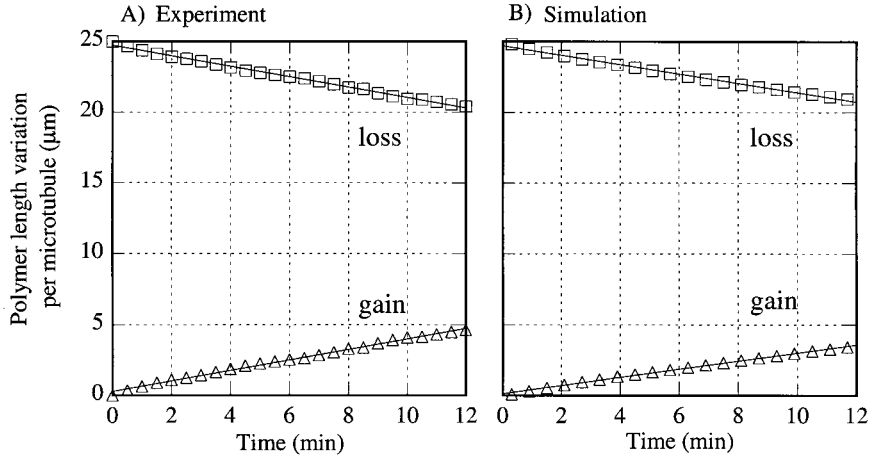

FIGURE 7 Loss of original polymer (*squares*) and gain of new polymer (*triangles*) as a function of time at steady-state assembly for (*A*) the experimentally measured 89 microtubules and (*B*) the Monte Carlo simulation of the assembly dynamics of 89 microtubules using the velocities and transition frequencies of dynamics instability measured for the experimental microtubules (Table 1). In each case, the loss and gains at each time point for plus and minus ends were calculated and summed together as described in the text. The thin lines are linear regression of the data, providing a gain (loss) rate of 0.37 (0.37) μm/min for the experiment and 0.29 (0.33) μm/min for the simulation.

crotubules. The unit of time in the simulation was 1 s. At each second interval, a random number was obtained to determine if a switch of state occurred. The probability of switching from the current state to a new state was calculated from the transition rates. For example, if an end was in growth, the probability that it would stay in growth was given by $1 - (k_{g-s} + k_{g-p})$. If the random number between 0 and 1 was less than this probability, then a switch occurred, if not, then growth occurred for a length given by the measured velocity of growth in 1 s. If a change of state resulted, then another random number was called to determine which of the two possible states occurred. Upon leaving growth, for example, an end could go to either shortening or pause. The probability of shortening, for example, was calculated from the ratio of the transition rate constants: $k_{g-s}/(k_{g-s} + k_{g-p})$. If the random number between 0 and 1 was less than this ratio, then a switch to shortening occurred, and the microtubule end lost length given by the velocity of shortening for one second. Otherwise the end entered the pause state and no change in length occurred.

A similar scheme was used for all three states of dynamic instability to model changes in length at plus and minus ends for 89 microtubules during a simulation period of 17 min, the mean duration of the experimental analysis. The

TABLE 1 Measured parameters of microtubule dynamic instability and polymer turnover near steady-state assembly

	Plus end	Minus end
Velocities (μm/min)		
Growth	0.70 ± 0.07	0.47 ± 0.08
Shortening	1.0 ± 0.2	0.6 ± 0.1
Fraction of time (%)		
Growth (f^g)	53	45
Shortening (f^s)	31	28
Pause (f^p)	16	27
Transition rate constant (min^{-1})		
k_{g-s}	0.17 ± 0.02	0.16 ± 0.02
k_{g-p}	0.06 ± 0.01	0.11 ± 0.02
k_{s-g}	0.28 ± 0.04	0.23 ± 0.03
k_{s-p}	0.04 ± 0.01	0.07 ± 0.02
k_{p-g}	0.14 ± 0.03	0.09 ± 0.01
k_{p-s}	0.08 ± 0.02	0.06 ± 0.01
Original polymer loss (μm/min)	0.26 ± 0.04	
Gain of new polymer (μm/min)	0.37 ± 0.06	

Dynamic instability parameters based on the three-state model described in Figure 8. Velocities of growth and shortening (± SEM) are measured from the respective positive and negative slopes in the time series. The fraction of time spent in the three states, growth (G), shrinkage (S), and pause (P), is given as percentage with respect to the total measurement time. The transition frequencies between three end states are described by the rate k_{i-j} = number of switches between state i and state j divided by the total time spent in i.

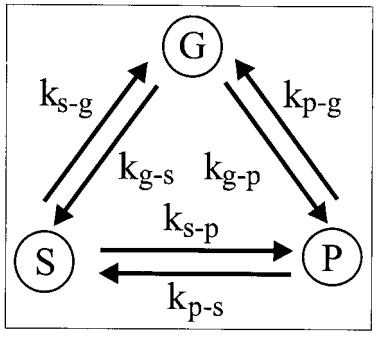

FIGURE 8 A three-state model that describes the dynamic instability of microtubule ends in the 2% glycerol assembly buffer. Each end was found to persist in either a growing state (G), a shortening state (S), or a pause state (P). The six transition rate constants k_{i-j} are the frequencies of transition from states i to j.

TABLE 2 Comparison of simulation and experimental results

	Simulation (%)	Experiment (%)
Total polymer length variation	2 ± 2	5
Fraction of population with:		
Plus end growth minus end shortening	26 ± 3	19 ± 5
Minus end growth plus end shortening	24 ± 3	34 ± 6
Growth at both ends	28 ± 5	37 ± 6
Shortening at both ends	21 ± 7	10 ± 3
Original polymer loss in 17 min	23 ± 2	18 ± 3
Gain of new polymer in 17 min	25 ± 5	24 ± 5

Comparison of microtubule assembly parameters obtained by the Monte Carlo simulation to those measured for the experimental microtubule population. Polymerization dynamics were simulated based on the parameters of dynamic instability and pause measured from the experimental polymerization (see Table 1) for the plus and minus ends of 89 microtubules for a period of 1000 s, the average duration of the experimental analysis. The final net growth or shortening of the plus and minus microtubule ends and the polymer turnover according to the simulation are compared with the results obtained in the assay.

simulation was begun with ends randomly chosen to be in a state of growth, shortening, or pause. Kinetic plots of individual ends as a function of simulation time were similar in variation to those shown for the experimental data in Fig. 5 (data not shown). The summary for the gain of new polymer and loss of old polymer at the plus and minus ends of each microtubule simulated is shown in Fig. 6 *B*. The random pattern is very similar to that of the experimental microtubules shown in Fig. 6 *A*. In addition, the simulation produced linear kinetics for the gain of new polymer and loss of original polymer at plus and minus ends for the population of microtubules (Fig. 7 *B*) much as occurs for the experimental microtubule population near steady state (Fig. 7 *A*). When microtubules dynamics was simulated for a long time, such as 160 min, the gain and loss rate progressively slowed down: in the first 12 min the rate was 0.3 μm/min, whereas, after 50 min, the gain rate reduced to 0.13 μm/min and the loss rate to even smaller value, 0.07 μm/min. The values given in Table 2 for the simulation are averages ± SEM for 10 runs of the simulation. The SEM reflects the effects of the stochastic variation in dynamic instability exhibited by different simulation runs. The simulations exhibited a 2% variation of the total polymer length between the beginning and the end of the simulation, as compared to 5% increment measured experimentally. The microtubule population was classified into four groups, according to the net plus- and minus-end growth or shortening at the end of the simulation or experiment. The fractions of the population falling into the four different classes according to the simulation were in agreement with the experimental results (Table 2).

DISCUSSION

The main conclusion we draw from our data is that, in general, polarized treadmilling (Fig. 1 *B*) is not exhibited by microtubules assembled to near steady state from pure tubulin using 2% glycerol to stabilize dynamic instability. For the 89 pure microtubules analyzed in our study, treadmilling, where the net assembly at one end equaled the net disassembly at the other, was a rare event. In contrast, an end appeared equally likely to achieve net growth or net shortening of variable length among the population of microtubules analyzed, although the total polymer remained nearly constant (Figs. 4, 5, and 6 *A*, Table 1). We did observe some treadmilling, but not unidirectionally: 34% of the microtubules achieved net growth at the minus end and net shortening at the plus end; and 19% of the population did the opposite. The remaining ones achieved net growth or shortening at both of their ends. These results indicate that the assembly behavior of individual microtubules depends mainly on stochastic differences in dynamic instability between the two ends (Fig. 1 *A*). This conclusion is verified by the nearly identical assembly behavior produced by Monte Carlo simulations of microtubule assembly using our measured parameters of dynamic instability for plus and minus ends (Fig. 6 *B* and Table 2). In our assay, we used kinesin motor proteins to bind microtubules to the coverslip surface and slowly translocate them in a minus direction to accurately identify polarity. It is unlikely that these motors had much influence on microtubule assembly because of the absence of polarity in the treadmilling behavior of the microtubules and because of the low motor density (less than 1–12 motors bound per 1625 dimers along a microtubule, as determined in the Materials and Methods).

There is another important aspect of both our measurements from individual microtubules and from the simulations based on their measured parameters of dynamic instability. They both predict the initial rates of original polymer loss and new polymer gain near steady-state assembly as reported by Panda et al. (1999) from their biochemical pulse-chase assays. Our measured rate of 0.37 μm/min for loss of original and gain of new polymer is very similar to the values measured by their biochemical assays: an average gain per microtubule of 0.32 ± 0.04 μm/min and an average loss of 0.26 ± 0.1 μm/min (Panda et al., 1999). Panda et al. did not measure the assembly behavior of individual microtubules at steady-state assembly as we did in our study, but instead inferred polarized treadmilling from their biochemical data and the suppression of dynamic instability produced by 2% glycerol in the assembly buffer. Our results show that polarized treadmilling is not required to explain the biochemical data; it can be produced by the stochastic variations in dynamic instability among the plus and minus ends of microtubules near steady-state assembly (Fig. 7, *A* and *B*). Because Panda et al. (1999) only report dynamic instability parameters for plus, but not minus ends, we were not able to use our computer simulations to test

predictions for loss of original and gain of new polymer based on their assays of individual microtubules.

Our data also excludes treadmilling produced by the Wegner mechanism as proposed by Panda et al. (1999). This is best seen by the equations used by Panda et al. in their treadmilling analysis, which describe assembly at plus and minus ends for the growth phase in the absence of a shortening phase,

$$dL^+/dt = k_2^{g+}(S - S_c^{g+}) = k_2^{g+}S - k_{-1}^{g+} \quad (1)$$

and

$$dL^-/dt = k_2^{g-}(S - S_c^{g-}) = k_2^{g-}S - k_{-1}^{g-}, \quad (2)$$

where dL/dt is the rate of change in length at an end, k_2^g is the second-order association rate constant, S is the steady-state tubulin dimer concentration, and S_c is the critical concentration, which is equal to the first-order dissociation of subunits from an end divided by the association rate constant ($S_c = k_{-1}^g/k_2^g$). Association depends on a second-order rate constant, but dissociation is independent of tubulin concentration as seen on the right side of Eqs. 1 and 2. Treadmilling will occur near steady-state assembly in a plus direction when S is maintained between the critical concentrations for the two ends with $S_c^- > S > S_c^+$. Under these conditions, the plus ends will grow and the minus ends will shorten in a balanced fashion at a rate given by Eqs. 1 and 2.

For treadmilling to be produced by the Wegner mechanism, the end with the higher critical concentration for growth must persist in disassembly while the other end with the lower critical concentration for growth persists in assembly. In our experiments, we found that neither the plus nor minus end persisted in disassembly; both ends were capable of growth. In their paper, Panda et al. (1999) did state that minus ends, like the measured plus ends, exhibited both the growth and shortening phases of dynamic instability. As a result, in both the Panda et al. experiments and ours, the tubulin concentration near steady-state assembly must have been greater than the critical concentrations for growth at either end ($S > S_c^+$ and $S > S_c^-$). Thus, treadmilling by the Wegner mechanism is not occurring for microtubules assembled from pure brain tubulin near steady-state assembly.

As initially described by Walker et al. (1988), treadmilling can potentially result from differences in the dynamic instability at opposite microtubule ends. For microtubule ends exhibiting dynamic instability and exhibiting rescue before complete depolymerization, Eqs. 1 and 2 can be expanded to include the contributions of the shortening phase produced by the loss of the GTP-tubulin stabilizing cap and the rapid dissociation of GDP-tubulin subunits (Walker et al., 1988),

$$dL^+/dt = f^{g+}k_2^{g+}(S - S_c^{g+}) - f^{s+}k_{-1}^{s+} = f^{g+}V^{g+} - f^{s+}V^{s+} \quad (3)$$

and

$$dL^-/dt = f^{g-}k_2^{g-}(S - S_c^{g-}) - f^{s-}k_{-1}^{s-} = f^{g-}V^{g-} - f^{s-}V^{s-}, \quad (4)$$

where f^g and f^s are the fractions of time spent in growth and shortening phases, respectively, $k_{-1}^s = V^s$ is the rate of GDP-tubulin dissociation in the shortening phase, and V^g is the velocity of growth, which equals $k_2^g(S - S_c^g)$. Note in Eqs. 3 and 4 that the velocity of growth depends on tubulin concentration, but the velocity of the shortening phase is independent of tubulin concentration (Walker et al., 1988). There are several parameters of dynamic instability, which, by their differences between plus and minus ends, could produce polarized treadmilling at steady-state assembly.

However, our measured dynamic instability parameters predict no polarized treadmilling consistent with our direct measurements. The time-averaged growth rate for plus ends was $f^{g+}V^{g+} = 0.37$ μm/min and for minus ends was $f^{g-}V^{g-} = 0.21$ μm/min. The time-averaged shortening rate at plus ends was $f^{s+}V^{s+} = 0.31$ μm/min and for minus ends was $f^{s-}V^{s-} = 0.17$ μm/min. Note that the fractions of time used in these calculations are the experimental values of time spent in growth normalized to the total time of observation (see Table 1). As a consequence, the predicted net assembly rate at the plus ends from Eq. 3 is 0.06 ± 0.06 μm/min, whereas the predicted net assembly rate at the minus ends is 0.04 ± 0.05 μm/min. Our measured length variation averaged over all the microtubules in our experimental population was 0.08 ± 0.04 μm/min for plus ends and 0.034 ± 0.02 μm/min for minus ends. These values are very close to the numbers predicted by the measured dynamic instability parameters. This analysis indicates that there is little difference in the net assembly rate of plus and minus ends near steady-state assembly and that the steady-state concentration is higher than the critical concentration of both ends, whatever their values.

Another approach to quantify the treadmilling effect, as proposed by Rodionov et al. (1999), expresses the fraction of growing ends as a function of tubulin concentration. Such fraction, or its equivalent, the probability that one end is in the growth phase, predicts net growth when larger than 0.5 and net disassembly when smaller than 0.5. In a system where treadmilling takes place, such as in the centrosome-free fibroblast cells described by Rodionov and co-workers (1997, 1999), the concentration of tubulin is such that the probability of growth of the plus end is close to 1 and the probability of growth of the minus end is close to 0. Such probability has been calculated for our experimental data as

$$P^g = f^gV^g/(f^gV^g + f^sV^s). \quad (5)$$

From the measured values in Table 1, Eq. 5 yields $P^{g+} = 0.54$ for the plus end and $P^{g-} = 0.55$ for the minus end, showing, once again, slight net assembly at both ends and

nearly the same value for both ends. From this and the above analysis, we conclude that microtubules assembled from pure brain tubulin in standard in vitro reassembly buffer containing 2% glycerol at 30°C exhibit no intrinsic polarized treadmilling on average.

Previously, Hotani and Horio (1988) directly visualized treadmilling of MAP-rich microtubules with addition at plus and loss at minus ends at a slow rate of 0.015 μm/min, as predicted by Bergen and Borisy (1980). This result was based on measurements of microtubules assembled with brain MAPs to suppress the shortening phases of dynamic instability and assumed that the plus ends were the fast-growing ends. These studies provide good evidence that MAPs, by suppressing rapid shortening phases at both ends, allow microtubules to treadmill by a Wegner mechanism. However, the steady-state concentration is very low and the treadmilling is very slow. This rate of treadmilling is far too slow to explain the 0.3 to 2 μm/min poleward flux of microtubules in the mitotic spindle or the 12 μm/min treadmilling observed by Rodionov and co-workers (1997, 1999) for interphase cytoplasmic microtubules within cytoplasts of mammalian tissue cells that have unusually high concentrations of free tubulin. To obtain the fast treadmilling rates observed in vivo, the requirement is not suppression of all dynamic instability, but a selective suppression of minus end growth and plus end shortening phases at the high tubulin concentrations needed for fast plus-end growth velocity.

This conclusion strengthens the hypothesis that polarized treadmilling or flux of microtubules in living cells is facilitated by non-tubulin factors that bias plus ends in growth and bias the minus ends in shortening (Mitchison, 1989; Waterman-Storer and Salmon, 1997a,b; Rodionov et al., 1999). The imaging assay we have developed can easily discriminate between stochastic treadmilling and a biased behavior. Possible molecular candidates for biasing plus- and minus-end dynamic instability include the catastrophe factors OP18/Stathmin (Howell et al., 1999), the catastrophic kinesin KinI (Desai et al., 1998), NEM-modified tubulins (Phelps and Walker, 2000), the minus-directed kinesin, Kar3 (Endow et al., 1994), and perhaps the activity of other microtubule motor proteins.

This work was supported by National Institutes of Health GM 60678 to E.D.S. We thank Dr. Michael Caplow for helpful discussions. S.G. would like to thank Paul S. Maddox and all the members of the Salmon Lab for their help and the nice environment in which this project was carried on.

REFERENCES

Bergen, L. G., and G. G. Borisy. 1980. Head-to-tail polymerization of microtubules in vitro. *J Cell Biol.* 84:141–150.

Desai, A., P. S. Maddox, T. J. Mitchison, and E. D. Salmon. 1998. Anaphase A chromosome movement and poleward spindle microtubule flux occur at the same rates in *Xenopus* extract spindles. *J. Cell Biol.* 141:703–713.

Desai, A., and T. J. Mitchison. 1997. Microtubule polymerization dynamics. *Ann. Rev. Cell Dev. Biol.* 13:83–117.

Duke, T., T. E. Holy, and S. Leibler. 1995. "Gliding assays" for motor proteins: a theoretical analysis. *Phys. Rev. Lett.* 74:330–333.

Endow, S., J. Kang Sang, L. L. Satterwhite, M. D. Rose, V. P. Skeen, and E. D. Salmon. 1994. Yeast Kar3 is a minus-end microtubule motor protein that destabilizes microtubules preferentially at the minus ends. *EMBO J.* 13:2708–2713.

Fygenson, D. K., E. Braun, and A. Libchaber. 1994. Phase diagram of microtubules. Pays. Rev. E 50:1579–1588.

Gildersleeve, R. F., A. R. Cross, K. E. Cullen, A. P. Fagen, and R. C. Williams. 1992. Microtubules grow and shorten at intrinsically variable rates. *J. Biol. Chem.* 267:7995–8006.

Hotani, H., and T. Horio. 1988. Dynamics of microtubules visualized by darkfield microscopy: treadmilling and dynamic instability. *Cell Motil. and Cytoskelet.* 10:229–236.

Howard, J., A. J. Hunt, and S. Baek. 1993. Assay of microtubule movement driven by single kinesin molecules. *Methods Cell Biol.* 39:138–147.

Howell, B., N. Larsson, M. Gullberg, and L. Cassimeris. 1999. Dissociation of the tubulin-sequestering and microtubule catastrophe-promoting activities of oncoprotein 18/Stathmin. *Mol. Biol. Cell.* 10:105–118.

Inoué, S., and E. D. Salmon. 1995. Force generation by microtubule assembly/disassembly in mitosis and related movements. *Mol. Biol. Cell.* 6:1619–1640.

Kristofferson, D., T. Michison, and M. Kirschner. 1986. Direct observation of steady-state microtubule dynamics. *J. Cell Biol.* 102:1007–1019.

Margolis, R. L. 1981. Role of GTP hydrolysis in microtubule treadmilling and assembly. *Proc. Natl. Acad. Sci. U.S.A.* 78:1586–1590.

Margolis, R. L., and L. Wilson. 1978. Opposite end assembly and disassembly of microtubules at steady state in vitro. *Cell.* 13:1–8.

Margolis, R. L., and L. Wilson. 1998. Microtubule treadmilling: what goes around come around. *Bioessays.* 20:830–836.

Mitchison, T. J. 1989. Polewards microtubule flux in the mitotic spindle: evidence from photoactivation of fluorescence. *J. Cell Biol.* 109: 637–652.

Michison, T., and M. Kirschner. 1984. Dynamic instability of microtubule growth. *Nature.* 312:237–242.

Mitchison, T. J., and E. D. Salmon. 1992. Poleward kinetochore fiber movement occurs during both metaphase and anaphase A in newt lung cell mitotis. *J. Cell Biol.* 119:569–582.

Panda, D., H. P. Miller, and L. Wilson. 1999. Rapid treadmilling of brain microtubules free of microtubule-associated proteins in vitro and its suppression by tau. *Proc. Natl. Acad. Sci. U.S.A.* 96:12459–12464.

Phelps, K. K., and R. A. Walker. 2000. NEM tubulin inhibits microtubule minus end assembly by a reversible capping mechanism. *Biochemistry.* 39:3877–3885.

Rodionov, V. I., and G. G. Borisy. 1997. Microtubule treadmilling in vivo. *Science.* 275:215–218.

Rodionov, V., E. Nadezhdina, and G. Borisy. 1999. Centrosomal control of microtubule dynamics. *Proc. Natl. Acad. Sci. U.S.A.* 96:115–120.

Toso, R. J., M. A. Jordan, K. W. Farrell, B. Matsumoto, and L. Wilson. 1993. Kinetic stabilization of microtubule dynamic instability in vitro by vinblastine. *Biochemistry.* 32:1285–1293.

Tran, P. T., P. Joshi, and E. D. Salmon. 1997a. How tubulin subunits are lost from the shortening ends of microtubules. *J. Struct. Biol.* 118: 107–118.

Tran, P. T., R. A. Walker, and E. D. Salmon. 1997b. A metastable intermediate state of microtubule dynamic instability that differs significantly between plus and minus ends. *J. Cell Biol.* 138:105–117.

Vasquez, R. J., B. Howell, A.-M. C. Yvon, P. Wadsworth, and L. Cassimeris. 1997. Nanomolar concentrations of nocodazole alter microtubule dynamic instability in vivo and in vitro. *Mol. Biol. Cell.* 8:973–985.

Walker, R. A., S. Inoué, and E. D. Salmon. 1989. Asymmetric behavior of severed microtubule ends after ultraviolet-microbeam irradiation of individual microtubules in vitro. *J. Cell Biol.* 108:931–937.

Walker, R. A., E. T. O'Brien, N. K. Pryer, M. F. Soboerio, W. A. Voter, H. P. Erickson, and E. D. Salmon. 1988. Dynamic instability of individual microtubules analyzed by video light microscopy: rate constants and transition frequencies. *J. Cell Biol.* 107:1437–1448.

Walker, R. A., N. K. Pryer, and E. D. Salmon. 1991. Dilution of individual microtubules observed in real time in vitro: evidence that cap size is small and independent of elongation rate. *J. Cell Biol.* 114:73–81.

Waterman-Storer, C. M., and E. D. Salmon. 1997a. Microtubule dynamics: treadmilling comes around again. *Curr. Biol.* 7:R369–R372.

Waterman-Storer, C. M., and E. D. Salmon. 1997b. Actomyosin-based retrograde flow of microtubules in the lamella of migrating epithelial cells influences microtubule dynamic instability and turnover and is associated with microtubule breakage and treadmilling. *J. Cell Biol.* 139:417–434.

Waterman-Storer, C. M., and E. D. Salmon. 1998. How microtubules get fluorescent speckles. *Biophys. J.* 75:2059–2069.

Waters, J. C., R. V. Skibbens, and E. D. Salmon. 1996. Oscillating mitotic newt lung cell kinetochores are, on average, under tension and rarely push. *J. Cell Sci.* 109:2823–2831.

Wegner, A. 1976. Head to tail polymerization of actin. *J. Mol. Biol.* 108:139–150.

Zhai, Y., P. J. Kronebusch, and G. G. Borisy. 1995. Kinetochore microtubule dynamics and the metaphase-anaphase transition. *J. Cell Biol.* 131:721–734.